

Chaotic behaviors of stable second-order digital filters with two's complement arithmetic

Bingo Wing-Kuen Ling, Wai-Fung Hung and Peter Kwong-Shun Tam

Department of Electronic and Information Engineering, The Hong Kong Polytechnic University, Hung Hom, Kowloon, Hong Kong, China

SUMMARY

In this paper, the behaviors of stable second-order digital filters with two's complement arithmetic are investigated. It is found that even though the poles are inside the unit circle and the trajectory converges to a fixed point on the phase plane, that fixed point is not necessarily the origin. That fixed point is found and the set of initial conditions corresponding to such trajectories is determined. This set of initial conditions is a set of polygons inside the unit square, whereas it is an ellipse for the marginally stable case. Also, it is found that the occurrence of limit cycles and chaotic fractal pattern on the phase plane can be characterized by the periodic and aperiodic behaviors of the symbolic sequences, respectively. The fractal pattern is polygonal, whereas it is elliptical for the marginally stable case.

KEY WORDS: stable; two's complement arithmetic; fractal pattern; limit cycles

1. INTRODUCTION

It is well known that chaotic behaviors may occur if second-order digital filters with two's complement arithmetic are operating in the marginally stable region or in the unstable region [1,4,6-10,12,13]. Further results have been reported for marginally stable third-order digital filters with two's complement arithmetic [3,13], as well as for marginally stable second-order digital filters with either a saturation-type nonlinearity [2] or with a quantization-type nonlinearity [5,11].

However, we seldom design a 'digital filter' operating in the marginally stable region or in the unstable region. Practically, we usually design digital filters operating in the stable region. In this paper, chaotic and related behaviors of stable second-order digital filters with two's complement arithmetic are investigated.

If overflow does not occur, the trajectory of stable second-order digital filters with two's complement arithmetic will converge to the origin on the phase plane. If overflow occurs, will the trajectory converge? If so, what are the fixed points and the set of initial conditions such that the trajectories will converge to those fixed points? Besides, some researchers have reported that limit cycles may occur [14-19]. What is the relationship between the occurrence of limiting cycles and the behaviors of symbolic sequences? Moreover, are there any fractal patterns exhibited on the phase plane? If so, what is the difference between the shapes of fractal patterns for the stable and the marginally stable second-order digital filters?

In section 2, we will outline the notations which are essentially those used in the existing literatures [1-13]. In section 3, the behaviors of stable second-order digital filters with two's complement arithmetic are presented. Comparisons between the behaviors of stable and marginally stable second-order digital filters with two's complement arithmetic are discussed in section 4. Finally, concluding remarks are presented in section 5.

2. NOTATIONS

The notations used in [1-13] are adopted as follows:

The system is defined as:

$$\begin{bmatrix} x_1(k+1) \\ x_2(k+1) \end{bmatrix} = F\left(\begin{bmatrix} x_1(k) \\ x_2(k) \end{bmatrix}\right) = \begin{bmatrix} x_2(k) \\ f(b \cdot x_1(k) + a \cdot x_2(k)) \end{bmatrix} = \mathbf{A} \cdot \begin{bmatrix} x_1(k) \\ x_2(k) \end{bmatrix} + \mathbf{B} \cdot s(k) \quad (1)$$

$$\text{where } \mathbf{x}(k) = \begin{bmatrix} x_1(k) \\ x_2(k) \end{bmatrix} \in I^2 \equiv \{(x_1, x_2) : -1 \leq x_1 < 1, -1 \leq x_2 < 1\} \quad (2)$$

$$\mathbf{A} = \begin{bmatrix} 0 & 1 \\ b & a \end{bmatrix} \quad (3)$$

$$\mathbf{B} = \begin{bmatrix} 0 \\ 2 \end{bmatrix} \quad (4)$$

$$s(k) \in \{-m, \dots, -1, 0, 1, \dots, m\} \text{ where } m \in \mathbb{Z}^+ \cup \{0\} \text{ satisfying} \\ -2 \cdot m - 1 \leq b \cdot x_1 + a \cdot x_2 < 2 \cdot m + 1 \quad (5)$$

$$\text{and } f(x) = x - 2 \cdot n \text{ for } 2 \cdot n - 1 \leq x < 2 \cdot n + 1 \text{ and } n \in \mathbb{Z}^+ \cup \{0\} \quad (6)$$

For the linearized model of the system, if $(a, b) \in \Delta \equiv \{(a, b) : b > -1 \text{ and } b < -a + 1 \text{ and } b < a + 1\}$, the second-order digital filters are said to be operating in the

stable region. If $b = -1$ and $|a| < 2$, or $b = a + 1$ and $-2 < a < 0$, or $b = -a + 1$ and $0 < a < 2$, the second-order digital filters are said to be operating in the marginally stable region. Otherwise, the second-order digital filters are said to be operating in the unstable region.

Given an initial condition $\mathbf{x}(0) \in I^2$, a symbolic sequence $s = (s(0), s(1), \dots) \in \Sigma$ can be generated by the map $S: I^2 \rightarrow \Sigma$. The set Σ can be partitioned into three subsets: $\Sigma_\alpha = \{s = (s(0), s(1), \dots) : s \text{ is periodic}\}$, $\Sigma_\beta = \{s = (s(0), s(1), \dots) : s \text{ is eventually periodic}\}$ and $\Sigma_\gamma = \Sigma \setminus (\Sigma_\alpha \cup \Sigma_\beta)$.

3. BEHAVIORS OF STABLE SECOND-ORDER DIGITAL FILTERS WITH TWO'S COMPLEMENT ARITHMETIC

This section presents the behaviors of stable second-order digital filters with two's complement arithmetic as follows:

3.1. Trajectory converging to the origin

In this section, the trajectory equation and the set of initial conditions for the trajectory to converge to the origin are discussed as below:

Consider the case when the eigenvalues of matrix \mathbf{A} are complex; let

$$b = -r^2 \text{ and } a = 2 \cdot r \cdot \cos \theta \quad (7)$$

$$\text{where } r \in \mathfrak{R}^+ \text{ and } \theta \in \mathfrak{R} \quad (8)$$

If $0 < r < 1$, then the second-order digital filters are stable.

$$\text{Let } \mathbf{D} = \begin{bmatrix} r \cdot e^{j\theta} & 0 \\ 0 & r \cdot e^{-j\theta} \end{bmatrix} \quad (9)$$

$$\mathbf{T} = \begin{bmatrix} \frac{1}{\sqrt{r}} \cdot e^{-\left(\frac{j\theta}{2}\right)} & \frac{1}{\sqrt{r}} \cdot e^{\frac{j\theta}{2}} \\ \sqrt{r} \cdot e^{\frac{j\theta}{2}} & \sqrt{r} \cdot e^{-\left(\frac{j\theta}{2}\right)} \end{bmatrix} \quad (10)$$

$$\text{Then } \mathbf{A} = \mathbf{T} \cdot \mathbf{D} \cdot \mathbf{T}^{-1} \quad (11)$$

If overflow does not occur, then

$$\mathbf{x}(k) = \mathbf{T} \cdot \mathbf{D}^k \cdot \mathbf{T}^{-1} \cdot \mathbf{x}(0) = \begin{bmatrix} \frac{r^{k-1}}{\sin \theta} \cdot (\sin(k \cdot \theta) \cdot x_2(0) - r \cdot \sin((k-1) \cdot \theta) \cdot x_1(0)) \\ \frac{r^k}{\sin \theta} \cdot (\sin((k+1) \cdot \theta) \cdot x_2(0) - r \cdot \sin(k \cdot \theta) \cdot x_1(0)) \end{bmatrix}, \quad \forall k \geq 1 \quad (12)$$

$$\Rightarrow \lim_{k \rightarrow +\infty} \mathbf{x}(k) = \mathbf{0} \quad (13)$$

Hence, the state vector converges to zero and the phase trajectory converges to the origin. Figure 1a shows an example of the corresponding phase portrait.

$$\mathbf{x}(k) \in I^2 \Rightarrow \left| \frac{r^k}{\sin \theta} \cdot (\sin((k+1) \cdot \theta) \cdot x_2(0) - r \cdot \sin(k \cdot \theta) \cdot x_1(0)) \right| < 1, \quad \forall k \geq 0 \quad (14)$$

If $\sin((k+1) \cdot \theta) > 0$, then

$$\frac{r \cdot \sin(k \cdot \theta) \cdot x_1(0) - \left| \frac{\sin \theta}{r^k} \right|}{\sin((k+1) \cdot \theta)} < x_2(0) < \frac{r \cdot \sin(k \cdot \theta) \cdot x_1(0) + \left| \frac{\sin \theta}{r^k} \right|}{\sin((k+1) \cdot \theta)} \quad (15)$$

If $\sin((k+1) \cdot \theta) < 0$, then

$$\frac{r \cdot \sin(k \cdot \theta) \cdot x_1(0) - \left| \frac{\sin \theta}{r^k} \right|}{\sin((k+1) \cdot \theta)} > x_2(0) > \frac{r \cdot \sin(k \cdot \theta) \cdot x_1(0) + \left| \frac{\sin \theta}{r^k} \right|}{\sin((k+1) \cdot \theta)} \quad (16)$$

By defining $I_k^2 \equiv \left\{ \mathbf{x}(0) : \mathbf{x}(0) \in I^2 \text{ and } \left| \sin((k+1) \cdot \theta) \cdot x_2(0) - r \cdot \sin(k \cdot \theta) \cdot x_1(0) \right| < \left| \frac{\sin \theta}{r^k} \right| \right\}$,

$\forall k \geq 0$, we can characterize I_k^2 as the region bounded between two parallel straight lines in I^2 described by the inequalities (15) or (16).

Although the slope of the two parallel straight lines for I_k^2 is different for different values of k , the y-intercepts of these two lines move away from the origin as k increases. Hence, $\exists K \geq 0$ such that $I_k^2 = I^2$ for $k \geq K$. This implies that

$\exists K' \geq 0$ such that $K' \leq K$ and $\bigcap_{k=0}^{+\infty} I_k^2 = \bigcap_{k=0}^{K'} I_k^2 \subseteq I^2$. As a result, if overflow does not

occur, then $\mathbf{x}(0) \in \bigcap_{k=0}^{K'} I_k^2$. This set of initial conditions corresponds to a polygon on

the phase plane, and the number of sides of the polygon depends on the value of K' , as shown in figure 1b.

3.2. Trajectory converging to a fixed point not at the origin

In this section, the trajectory equation and the set of initial conditions when the trajectory converges to a fixed point not at the origin are developed and discussed as below:

$$\mathbf{x}(k+1) = \mathbf{A} \cdot \mathbf{x}(k) + \mathbf{B} \cdot s(k), \quad \forall k \geq 0 \quad (17)$$

If $s(k) = s_0$ for $\forall k \geq 0$, then (18)

$$\begin{aligned} \mathbf{x}(k) &= \mathbf{A}^k \cdot \mathbf{x}(0) + \sum_{n=0}^{k-1} \mathbf{A}^n \cdot \mathbf{B} \cdot s_0 \\ &= \begin{bmatrix} \frac{r^{k-1}}{\sin \theta} \cdot (\sin(k \cdot \theta) \cdot x_2(0) - r \cdot \sin((k-1) \cdot \theta) \cdot x_1(0)) \\ \frac{r^k}{\sin \theta} \cdot (\sin((k+1) \cdot \theta) \cdot x_2(0) - r \cdot \sin(k \cdot \theta) \cdot x_1(0)) \end{bmatrix}, \quad \forall k \geq 1 \\ &+ \frac{2 \cdot s_0}{\sin \theta \cdot (1 - 2 \cdot r \cdot \cos \theta + r^2)} \cdot \begin{bmatrix} \sin \theta - r^{k-1} \cdot \sin(k \cdot \theta) + r^k \cdot \sin((k-1) \cdot \theta) \\ \sin \theta - r^k \cdot \sin((k+1) \cdot \theta) + r^{k+1} \cdot \sin(k \cdot \theta) \end{bmatrix} \end{aligned} \quad (19)$$

Since $0 < r < 1$, we have $\lim_{k \rightarrow +\infty} \mathbf{x}(k) = \frac{2 \cdot s_0}{1 - 2 \cdot r \cdot \cos \theta + r^2} \cdot \begin{bmatrix} 1 \\ 1 \end{bmatrix}$ (20)

Let $\mathbf{x}^* = \frac{2 \cdot s_0}{1 - 2 \cdot r \cdot \cos \theta + r^2} \cdot \begin{bmatrix} 1 \\ 1 \end{bmatrix}$ (21)

Then $\mathbf{x}(k)$ will converge to \mathbf{x}^* . If $s_0 \neq 0$, then $\mathbf{x}^* \neq \mathbf{0}$. Hence, the trajectory converges to a fixed point not at the origin. Figure 2a shows an example of the corresponding phase portrait. In fact, when $s_0 = 0$, then $\mathbf{x}^* = \mathbf{0}$. This reduces to the case described in section 3.1.

$$\begin{aligned} \mathbf{x}(k) \in I^2 \Rightarrow & \left| \frac{r^k}{\sin \theta} \cdot (\sin((k+1) \cdot \theta) \cdot x_2(0) - r \cdot \sin(k \cdot \theta) \cdot x_1(0)) + \right. \\ & \left. \frac{2 \cdot s_0}{\sin \theta \cdot (1 - 2 \cdot r \cdot \cos \theta + r^2)} \cdot (\sin \theta - r^k \cdot \sin((k+1) \cdot \theta) + r^{k+1} \cdot \sin(k \cdot \theta)) \right| < 1, \quad \forall k \geq 0 \end{aligned} \quad (22)$$

If $\sin((k+1) \cdot \theta) > 0$, then

$$\begin{aligned} & - \left| \frac{\sin \theta}{r^k} \right| - \frac{2 \cdot s_0}{1 - 2 \cdot r \cdot \cos \theta + r^2} \cdot \left(\frac{\sin \theta}{r^k} - \sin((k+1) \cdot \theta) + r \cdot \sin(k \cdot \theta) \right) + r \cdot \sin(k \cdot \theta) \cdot x_1(0) \\ & \frac{\sin \theta}{r^k} - \frac{2 \cdot s_0}{1 - 2 \cdot r \cdot \cos \theta + r^2} \cdot \left(\frac{\sin \theta}{r^k} - \sin((k+1) \cdot \theta) + r \cdot \sin(k \cdot \theta) \right) + r \cdot \sin(k \cdot \theta) \cdot x_1(0) \\ & \frac{\sin \theta}{r^k} - \frac{2 \cdot s_0}{1 - 2 \cdot r \cdot \cos \theta + r^2} \cdot \left(\frac{\sin \theta}{r^k} - \sin((k+1) \cdot \theta) + r \cdot \sin(k \cdot \theta) \right) + r \cdot \sin(k \cdot \theta) \cdot x_1(0) \\ & \frac{\sin \theta}{r^k} - \frac{2 \cdot s_0}{1 - 2 \cdot r \cdot \cos \theta + r^2} \cdot \left(\frac{\sin \theta}{r^k} - \sin((k+1) \cdot \theta) + r \cdot \sin(k \cdot \theta) \right) + r \cdot \sin(k \cdot \theta) \cdot x_1(0) \end{aligned} \quad (23)$$

If $\sin((k+1) \cdot \theta) < 0$, then

$$\begin{aligned}
& - \frac{\left| \frac{\sin \theta}{r^k} \right| - \frac{2 \cdot s_0}{1 - 2 \cdot r \cdot \cos \theta + r^2} \cdot \left(\frac{\sin \theta}{r^k} - \sin((k+1) \cdot \theta) + r \cdot \sin(k \cdot \theta) \right) + r \cdot \sin(k \cdot \theta) \cdot x_1(0)}{\sin((k+1) \cdot \theta)} \\
& > x_2(0) > \\
& \frac{\left| \frac{\sin \theta}{r^k} \right| - \frac{2 \cdot s_0}{1 - 2 \cdot r \cdot \cos \theta + r^2} \cdot \left(\frac{\sin \theta}{r^k} - \sin((k+1) \cdot \theta) + r \cdot \sin(k \cdot \theta) \right) + r \cdot \sin(k \cdot \theta) \cdot x_1(0)}{\sin((k+1) \cdot \theta)}
\end{aligned} \tag{24}$$

By defining $I'_{k,s_0}{}^2 \equiv \left\{ \mathbf{x}(0) : \mathbf{x}(0) \in I^2 \text{ and } \left| \frac{r^k}{\sin \theta} \cdot (\sin((k+1) \cdot \theta) \cdot x_2(0) - r \cdot \sin(k \cdot \theta) \cdot x_1(0)) + \frac{2 \cdot s_0}{\sin \theta \cdot (1 - 2 \cdot r \cdot \cos \theta + r^2)} \cdot (\sin \theta - r^k \cdot \sin((k+1) \cdot \theta) + r^{k+1} \cdot \sin(k \cdot \theta)) \right| < 1 \right\}$, $\forall k \geq 0$ and

$\forall s_0 \neq 0$, we can characterize $I'_{k,s_0}{}^2$ as the region bounded between two parallel

straight lines in I^2 described by the inequalities (23) or (24). Similarly, $\exists K'_{s_0} \geq 0$

such that $\bigcap_{k=0}^{+\infty} I_{k,s_0}{}^2 = \bigcap_{k=0}^{K'_{s_0}} I_{k,s_0}{}^2 \subseteq I^2$. As a result, if $s(k) = s_0 \neq 0$ for $\forall k \geq 0$, then

$\mathbf{x}(0) \in \bigcup_{\forall s_0 \neq 0} \bigcap_{k=0}^{K'_{s_0}} I'_{k,s_0}{}^2$. This set of initial conditions also corresponds to some polygons

on the phase plane, with each polygon associated with a particular value of s_0 and the number of sides of the polygon depends on the value of K'_{s_0} , as shown in figure 2b.

3.3. Occurrence of limit cycles

In this section, the relationship between the occurrence of limit cycles and the periodic behaviors of the symbolic sequences is developed and discussed as follows:

$$\forall p, M \in \mathbb{Z}^+ \text{ and } \forall k \geq 0, \mathbf{x}(k + p \cdot M) = \mathbf{A}^{p \cdot M} \cdot \mathbf{x}(k) + \sum_{n=0}^{p \cdot M - 1} \mathbf{A}^{p \cdot M - 1 - n} \cdot \mathbf{B} \cdot s(k + n) \tag{25}$$

If $\exists k_0 \geq 0$ and $\exists M \in \mathbb{Z}^+$ such that $s(k) = s(k + M)$ for $\forall k \geq k_0$, that is $s \in \Sigma_\alpha \cup \Sigma_\beta$,

then $\forall p \in \mathbb{Z}^+$ (26)

$$\mathbf{x}(k_0 + p \cdot M) = \mathbf{T} \cdot \mathbf{D}^{p \cdot M} \cdot \mathbf{T}^{-1} \cdot \mathbf{x}(k_0) + \sum_{n=0}^{M-1} \mathbf{T} \cdot \mathbf{D}^{M-1-n} \cdot \left(\sum_{m=0}^{p-1} \mathbf{D}^{m \cdot M} \right) \cdot \mathbf{T}^{-1} \cdot \mathbf{B} \cdot s(k_0 + n) \tag{27}$$

$$= \mathbf{T} \cdot \mathbf{D}^{p \cdot M} \cdot \mathbf{T}^{-1} \cdot \mathbf{x}(k_0) + \sum_{n=0}^{M-1} \mathbf{T} \cdot \begin{bmatrix} \frac{r^{M-1-n} \cdot e^{j(M-1-n)\theta} \cdot (1 - r^{p \cdot M} \cdot e^{j \cdot p \cdot M \cdot \theta})}{1 - r^M \cdot e^{j \cdot M \cdot \theta}} & 0 \\ 0 & \frac{r^{M-1-n} \cdot e^{-j(M-1-n)\theta} \cdot (1 - r^{p \cdot M} \cdot e^{-j \cdot p \cdot M \cdot \theta})}{1 - r^M \cdot e^{-j \cdot M \cdot \theta}} \end{bmatrix} \cdot \mathbf{T}^{-1} \cdot \mathbf{B} \cdot s(k_0 + n) \quad (28)$$

$$\lim_{p \rightarrow +\infty} \mathbf{x}(k_0 + p \cdot M) = \sum_{n=0}^{M-1} \mathbf{T} \cdot \begin{bmatrix} \frac{r^{M-1-n} \cdot e^{j(M-1-n)\theta}}{1 - r^M \cdot e^{j \cdot M \cdot \theta}} & 0 \\ 0 & \frac{r^{M-1-n} \cdot e^{-j(M-1-n)\theta}}{1 - r^M \cdot e^{-j \cdot M \cdot \theta}} \end{bmatrix} \cdot \mathbf{T}^{-1} \cdot \mathbf{B} \cdot s(k_0 + n) \quad (29)$$

$$\text{Let } \mathbf{x}_0^* = \sum_{n=0}^{M-1} \mathbf{T} \cdot \begin{bmatrix} \frac{r^{M-1-n} \cdot e^{j(M-1-n)\theta}}{1 - r^M \cdot e^{j \cdot M \cdot \theta}} & 0 \\ 0 & \frac{r^{M-1-n} \cdot e^{-j(M-1-n)\theta}}{1 - r^M \cdot e^{-j \cdot M \cdot \theta}} \end{bmatrix} \cdot \mathbf{T}^{-1} \cdot \mathbf{B} \cdot s(k_0 + n) \quad (30)$$

$$\text{By defining } \mathbf{x}_n^* = \mathbf{A}^n \cdot \mathbf{x}_0^* + \sum_{m=0}^{n-1} \mathbf{A}^{n-1-m} \cdot \mathbf{B} \cdot s(k_0 + m) \text{ for } n=1, 2, \dots, M-1 \quad (31)$$

then $\mathbf{x}(k)$ will converge to a periodic sequence $\{\mathbf{x}_0^*, \mathbf{x}_1^*, \dots, \mathbf{x}_{M-1}^*\}$. Hence, limit cycles with period M will occur. Figure 3a and figure 3b shows an example of the corresponding phase portrait and the set of initial conditions that generate limiting cycles, respectively.

3.4. Chaotic fractal pattern

In this section, we demonstrate by simulation that when the symbolic sequences are aperiodic, that is, $s \in \Sigma_\gamma$, stable second-order digital filters with two's complement arithmetic may also exhibit a chaotic fractal pattern on the phase plane. The fractal pattern is polygonal, whereas it is elliptical for the marginally stable case. Figure 4a shows an example of the corresponding phase portrait.

Define $\Xi_0 \equiv \{\mathbf{x}(0) : s(k) = 0, \forall k \geq k_0\}$. This set is the set of initial conditions that the state trajectories will converge to zero. When $k_0 = 0$, we have found that

$$\Xi_0 = \bigcap_{k=0}^{K'} I_k^2. \text{ Similarly, define } \Xi_1 \equiv \{\mathbf{x}(0) : s(k) = s_0 \neq 0, \forall k \geq k_0^1\}. \text{ This set is the set of}$$

initial conditions that the state trajectories will converge to a fixed point. When

$$k_0^1 = 0, \text{ we have found that } \Xi_1 = \bigcup_{\forall s_0 \neq 0} \bigcap_{k=0}^{K'_{s_0}} I'_{k, s_0}{}^2. \text{ Likewise, we define}$$

$\Xi_M \equiv \{\mathbf{x}(0) : s(k) = s(k+M), \text{ for } k \geq k_0^M \text{ and for } M > 1\}$. This set is the set of initial

conditions that generates limiting cycles. If $\Xi_3 = I^2 \setminus \bigcup_{M \geq 0} \Xi_M \neq \emptyset$, this implies that there exists some initial conditions which may not result in the convergence of the state trajectories nor the occurrence of limiting cycles. Under this condition, chaotic behaviors may occur.

Since $\forall k \geq 0$, $\mathbf{x}(k)$ will not fall into the set $\bigcup_{M \geq 0} \Xi_M$, otherwise, $\exists k_0 \geq 0$ such that $\mathbf{x}(k_0) \in \bigcup_{M \geq 0} \Xi_M$. As a result, the phase portrait is inside $\Xi_3 = I^2 \setminus \bigcup_{M \geq 0} \Xi_M$. This may correspond to polygonal fractal patterns because $\Xi_M \quad \forall M \geq 0$ are all polygons. Figure 4b shows an example of the set of initial conditions that gives polygonal fractal patterns.

4. COMPARISONS BETWEEN THE BEHAVIORS OF STABLE AND MARGINALLY STABLE SECOND-ORDER DIGITAL FILTERS WITH TWO'S COMPLEMENT ARITHMETIC

Table 1 summarizes the differences on the behaviors of the state trajectories $\mathbf{x}(k)$ between stable and marginally stable second-order digital filters with two's complement arithmetic. Table 2 summarizes the corresponding differences on the phase portrait. Table 3 summarizes the differences on the sets of initial conditions for the occurrence of various symbolic sequences between stable and marginally stable second-order digital filters with two's complement arithmetic.

	$s(k) = 0,$ $\forall k \geq 0$	$s(k) = s_0 \neq 0,$ $\forall k \geq 0$	$s \in \Sigma_\alpha \cup \Sigma_\beta$	$s \in \Sigma_\gamma$
state trajectory $\mathbf{x}(k)$ of marginally stable second-order digital filters with two's complement arithmetic	oscillates with its natural frequency, and the DC value=0	oscillates with its natural frequency, and the DC value \neq 0	oscillates with harmonic frequencies $\frac{2 \cdot \pi \cdot n}{M}$, for $n = 0, 1, \dots, M - 1$	chaotic

state trajectory $\mathbf{x}(k)$ of stable second-order digital filters with two's complement arithmetic	converges to zero	converges to a non-zero value	limit cycles occur with period M	chaotic
--	-------------------	-------------------------------	------------------------------------	---------

Table 1. Comparison of the behaviors of state trajectories $\mathbf{x}(k)$ between stable and marginally stable second-order digital filters with two's complement arithmetic, for the initial conditions in Table 3.

	$s(k) = 0,$ $\forall k \geq 0$	$s(k) = s_0 \neq 0,$ $\forall k \geq 0$	$s \in \Sigma_\alpha \cup \Sigma_\beta$	$s \in \Sigma_\gamma$
phase portrait of marginally stable second-order digital filters with two's complement arithmetic	single ellipse centered at the origin	several ellipses with same size, and all the centers are not at the origin	several ellipses with different sizes, and all the centers are not at the origin	elliptical fractal pattern
phase portrait of stable second-order digital filters with two's complement arithmetic	converges to the origin	converges to a fixed point, and the fixed point is not at the origin	converges to several fixed points, and those fixed points are not at the origin	polygonal fractal pattern

Table 2. Comparison of the phase portraits between stable and marginally stable second-order digital filters with two's complement arithmetic, for the initial conditions in Table 3.

	$s(k) = 0,$ $\forall k \geq 0$	$s(k) = s_0 \neq 0,$ $\forall k \geq 0$	$s \in \Sigma_\alpha \cup \Sigma_\beta$	$s \in \Sigma_\gamma$
set of initial conditions of marginally stable second-order digital filters with two's complement arithmetic	single ellipse centered at the origin	several ellipses with same size, and all the centers are not at the origin	several ellipses with different sizes, and all the centers are not at the origin	elliptical fractal pattern
set of initial conditions of stable second-order digital filters with two's complement arithmetic	single polygon centered at the origin	several polygons with same size, and all the centers are not at the origin	several polygons with different sizes, and all the centers are not at the origin	polygonal fractal pattern

Table 3. Comparison of the sets of initial conditions for the occurrence of various symbolic sequences between stable and marginally stable second-order digital filters with two's complement arithmetic.

5. CONCLUDING REMARKS

In this paper, we have studied the behaviors of stable second-order digital filters with two's complement arithmetic. It is found that the state vector of stable second-order digital filters with two's complement arithmetic may not converge to zero. The sets of initial conditions that the trajectories converge to those fixed points are polygons inside the unit square. Also, it is found that the occurrence of limit cycles and chaotic fractal patterns on the phase plane can be characterized by the periodic and aperiodic behaviors of the symbolic sequences, respectively. The fractal pattern is polygonal, whereas it is elliptical for the marginally stable case.

ACKNOWLEDGEMENT

The work described in this paper was substantially supported by The Hong Kong Polytechnic University.

REFERENCES

1. Chua LO, Lin T. Chaos in digital filters. *IEEE Transactions on Circuits and Systems* 1988; **35**(6):648-658.
2. Galias Z, Ogorzalek MJ. Bifurcation phenomena in second-order digital filter with saturation-type adder overflow characteristic. *IEEE Transactions on Circuits and Systems* 1990; **37**(8):1068-1070.
3. Chua LO, Lin T. Chaos and fractals from third-order digital filters. *International Journal of Circuit Theory and Applications* 1990; **18**:241-255.
4. Chua LO, Lin T. Fractal pattern of second-order non-linear digital filters: a new symbolic analysis. *International Journal of Circuit Theory and Applications* 1990; **18**:541-550.
5. Lin T, Chua LO. On chaos of digital filters in the real world. *IEEE Transactions on Circuits and Systems* 1991; **38**(5):557-558.
6. Galias Z, Ogorzalek MJ. On symbolic dynamics of a chaotic second-order digital filter. *International Journal of Circuit Theory and Applications* 1992; **20**:401-409.
7. Wu CW, Chua LO. Properties of admissible symbolic sequences in a second-order digital filter with overflow non-linearity. *International Journal of Circuit Theory and Applications* 1993; **21**:299-307.
8. Kocarev L, Chua LO. On chaos in digital filters: case $b=-1$. *IEEE Transactions on Circuits and Systems—II: Analog and Digital Signal Processing* 1993; **40**(6):404-407.
9. Kocarev L, Wu CW, Chua LO. Complex behavior in digital filters with overflow nonlinearity: analytical results. *IEEE Transactions on Circuits and Systems—II: Analog and Digital Signal Processing* 1996; **43**(3):234-246.
10. Yu X, Galias Z. Periodic behaviors in a digital filter with two's complement arithmetic. *IEEE Transactions on Circuits and Systems—I: Fundamental Theory and Applications* 2001; **48**(10):1177-1190.
11. Ling BWK, Luk FCK, Tam PKS. Further investigation on chaos of real digital filters. *International Journal of Bifurcation and Chaos* 2003; **13**(2):493-495.
12. Ling WK, Tam PKS. Some new trajectory patterns and periodic behaviors of unstable second-order digital filter with two's complement arithmetic. *International Journal of Bifurcation and Chaos* 2003; **13**(9).
13. Ling WK, Hung WF, Tam PKS. Chaotic behaviors of a digital filter with two's complement arithmetic and arbitrary initial conditions and order. *International Journal of Bifurcation and Chaos* 2004; **14**(7).

14. Sandberg IW, Kaiser JF. A bound on limit cycles in fixed-point implementations of digital filters. *IEEE Transactions on Audio and Electroacoustics* 1972; **AU-20**(2):110-112.
15. Parker SR, Hess SF. Limit-cycle oscillations in digital filters. *IEEE Transactions on Circuit Theory* 1971; **CT-18**(6):687-697.
16. Thông T, Liu B. Limit cycles in the combinatorial implementation of digital filters. *IEEE Transactions on Acoustics, Speech, and Signal Processing* 1976; **ASSP-24**(3):248-256.
17. Barnes CW, Fam AT. Minimum norm recursive digital filters that are free of overflow limit cycles. *IEEE Transactions on Circuits and Systems* 1977; **CAS-24**(10):569-574.
18. Mills WL, Mullis CT, Roberts RA. Digital filter realizations without overflow oscillations. *IEEE Transactions on Acoustics, Speech, and Signal Processing* 1978; **ASSP-26**(4):334-338.
19. Munson DC, Strickland JH, Walker TP. Maximum amplitude zero-input limit cycles in digital filters. *IEEE Transactions on Circuits and Systems* 1984; **CAS-31**(3):266-275.

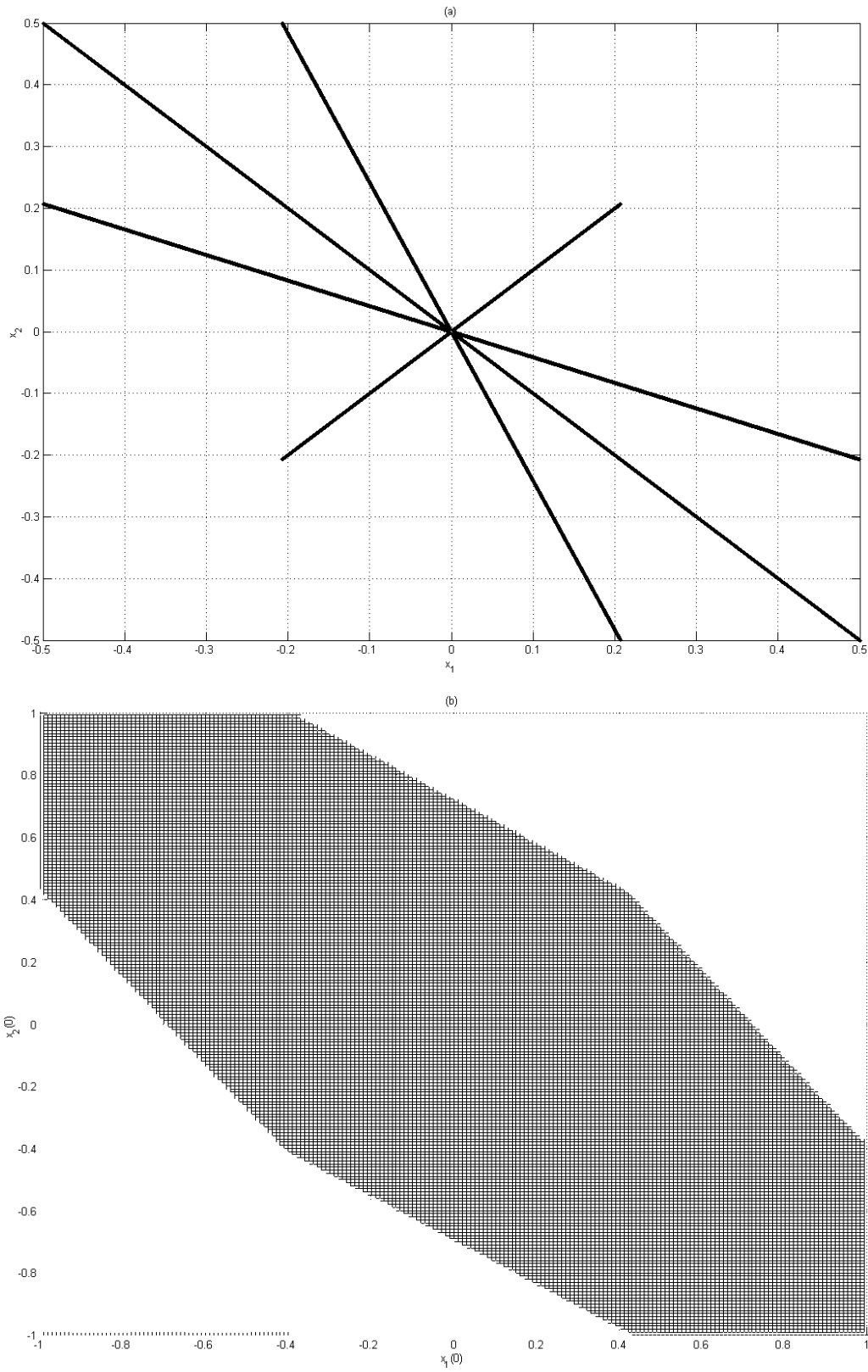


Figure 1. (a) The phase portrait of stable second-order digital filters with two's complement arithmetic, $r = 0.9999$, $\theta = 0.75 \cdot \pi$ and $\mathbf{x}(0) = \begin{bmatrix} 0.5 \\ -0.5 \end{bmatrix}$. (b) The set of initial conditions of the corresponding digital filters when $s(k) = 0 \quad \forall k \geq 0$.

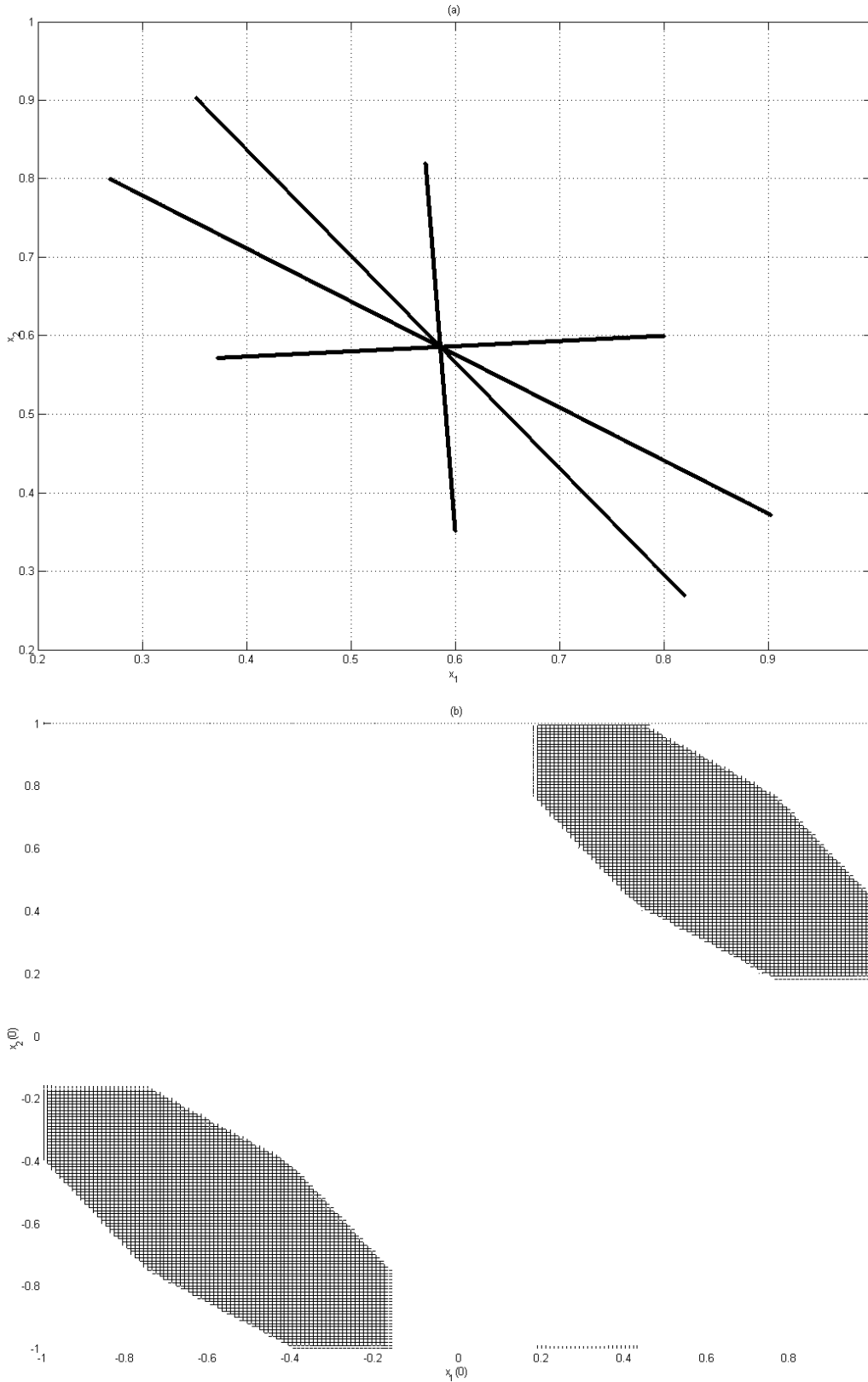


Figure 2. (a) The phase portrait of stable second-order digital filters with two's complement arithmetic, $r = 0.9999$, $\theta = 0.75 \cdot \pi$ and $\mathbf{x}(0) = \begin{bmatrix} 0.8 \\ 0.6 \end{bmatrix}$. (b) The set of initial conditions of the corresponding digital filters when $s(k) = s_0 \neq 0 \quad \forall k \geq 0$.

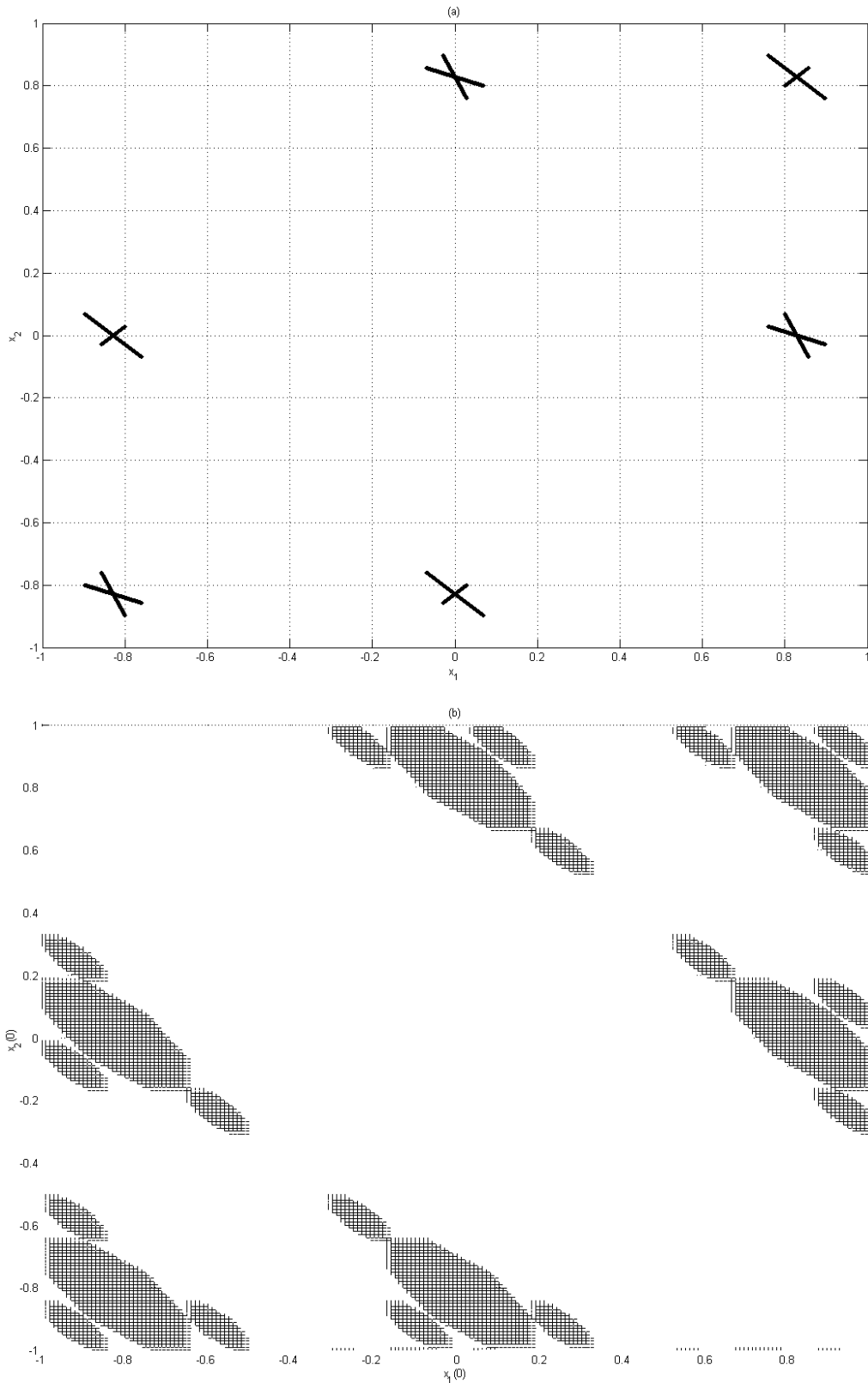


Figure 3. (a) The phase portrait of stable second-order digital filters with two's complement arithmetic, $r = 0.9999$, $\theta = 0.75 \cdot \pi$ and $\mathbf{x}(0) = \begin{bmatrix} 0.8 \\ 0.6 \end{bmatrix}$. (b) The set of initial conditions of the corresponding digital filters when $s(k) = s(k + M) \quad \forall k \geq 0$.

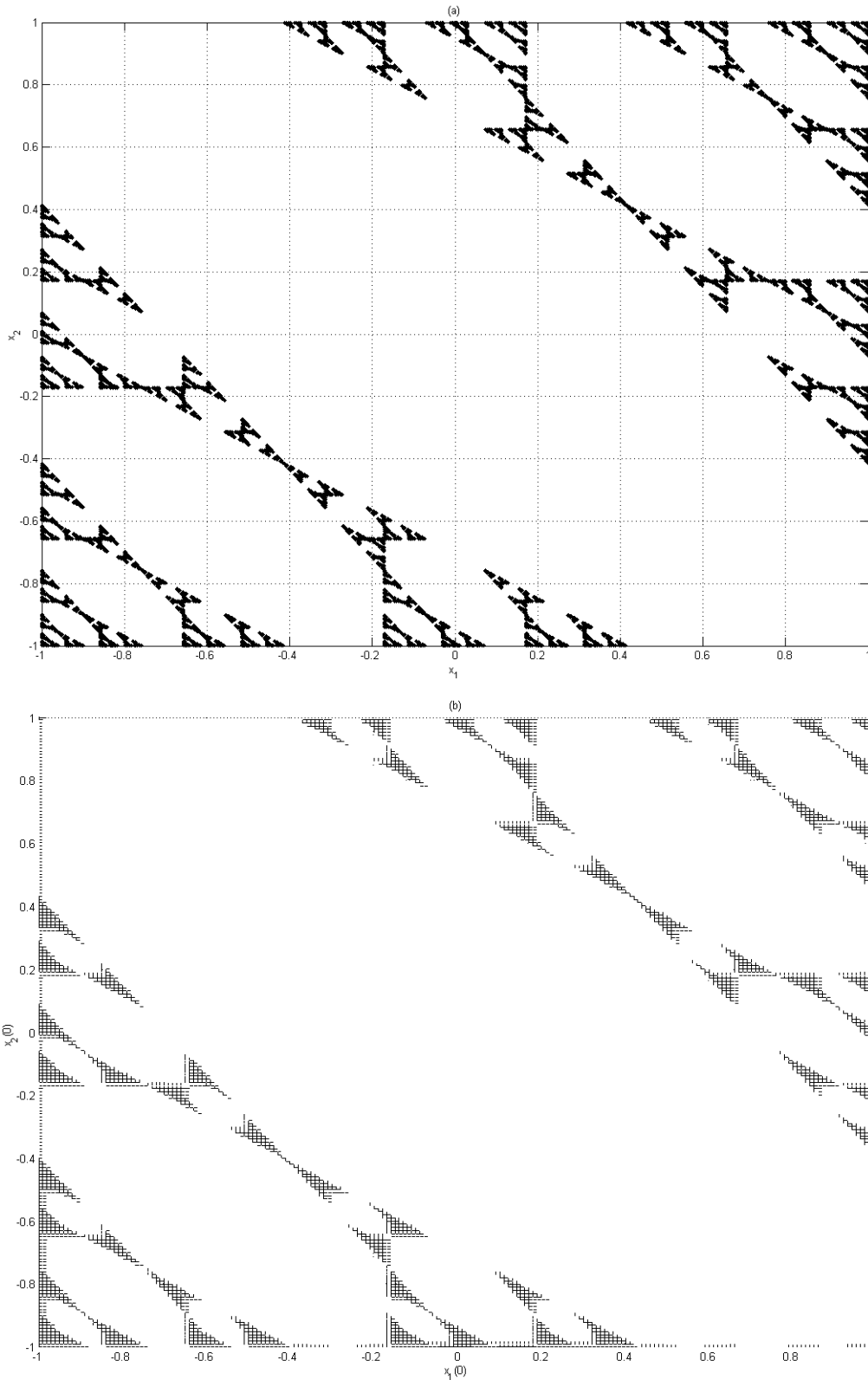


Figure 4. (a) The phase portrait of stable second-order digital filters with two's complement arithmetic, $r = 0.9999$, $\theta = 0.75 \cdot \pi$ and $\mathbf{x}(0) = \begin{bmatrix} -1 \\ 0 \end{bmatrix}$. (b) The set of initial conditions of the corresponding digital filters when $s(k)$ is aperiodic.